KERNFORSCHUNGSZENTRUM

KARLSRUHE

Potential Landscape for Fissioning Nuclei
I. General Method, Symetric Shapes

B. L. Andersen, F. Dickmann, K. Dietrich

2.J

POTENTIAL LANDSCAPE FOR FISSIONING NUCLEI

(I). General method, symmetric shapes

B. L. ANDERSEN

The Niels Bohr Institute, Copenhagen

FRIEDRICH DICKMANN

Kernforschungszentrum Karlsruhe

and

KLAUS DIETRICH

Institute for Theoretical Physics, University of Heidelberg and Kernforschungszentrum Karlsruhe

Abstract: The potential energy of a nucleus is calculated as a function of its shape using the method of Strutinski. The nuclear shapes are composed of two spheroids (centres $z = \pm z_1$; z-axis = symmetry axis) smoothly joined by a central hyperboloid (neck) or a central spheroid (belly). The corresponding shell-model potential is constructed from two harmonic oscillators centered around $z = \pm z_1$ and smoothly joined by a third oscillator centered around $z = 0$. A generalized form of Nilssons's spin-orbit and l^2 term is used.

1. Introduction

As a first step towards the understanding of nuclear fission, shape isomerism and related phenomena, one studies the "deformation energy" i.e. the difference between the total intrinsic energy of the nucleus having some given shape minus the total intrinsic energy of the same nucleus having a spherical shape. In determining the energy of strongly deformed nuclei we have to account for saturation as the basic property of nuclear matter. Since, furthermore, we are mainly concerned with the deformation energy of *heavy*, fissile nuclei, the liquid drop model (LDM) suggests itself as an adequate basis of a phenomenological description. Many calculations of the deformation energy within the LDM have been performed since the basic paper of Bohr and Wheeler [1]) with various degrees of sophistication as to the LDM and the variety of investigated nuclear shapes [2-5]). In the early sixties, it was realized that the nuclear shell structure which leads to fluctuations of the actual nuclear density around the constant liquid drop value, creates a significant modification of the LD energies. Myers and Swiatecki [6]) achieved a remarkable improvement of the LD mass formula by adding a shell correction term which depends on the difference of the actual density of shell-model levels from a smooth average level distribution. This shell correction term is constructed such as to tend to zero at large deformation. Strutinski [7]) showed that the effect of the shell structure was directly related to the fluctuation of

337

the nuclear density and that it could lead to an important modification of the LD energy at small as well as large deformations. The "Strutinski prescription" of calculating the shell correction term gives rise to a very successful parameterization of ground state masses [8]) and predicts the existence of nuclear shape isomers. It has consequently been widely adopted as a phenomenological method for calculating the deformation energy of heavy fissioning nuclei. The various groups of authors differ in the choice of the shell-model potential and the parametrization of nuclear shapes.
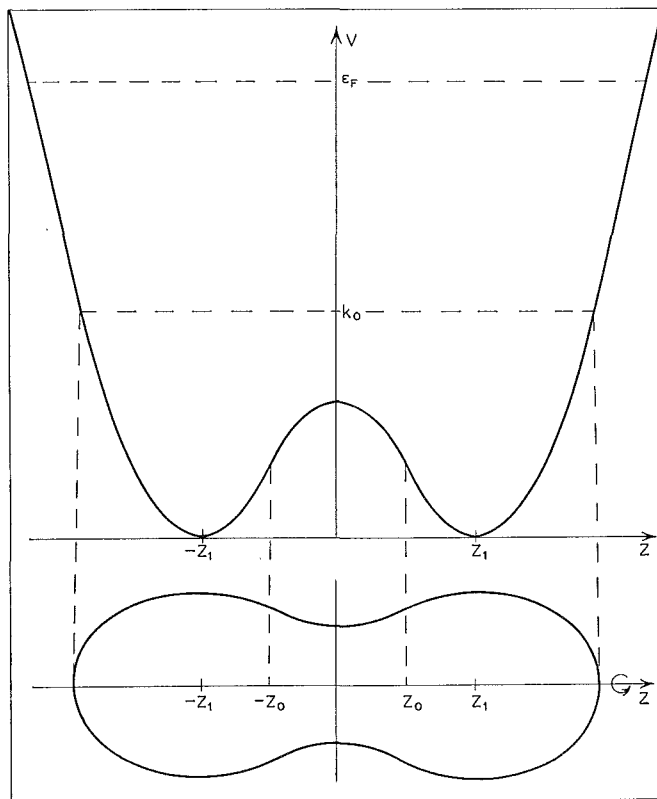
Fig. 1. Potential $V(z)$ for a given nuclear shape. If not otherwise mentioned, the input parameters in all the figures are the ones given in sect. 3.

Hitherto, only nuclear shapes with rotational symmetry around a body-fixed axis (z-axis) have been considered in this way. Furthermore, most of the calculations were restricted to nuclear shapes which are invariant against reflection with respect to a plane perpendicular to the axis of rotational symmetry. We shall shortly designate shapes with this additional symmetry as symmetric shapes contrary to asymmetric shapes.

Strutinski *et al.* [9]) use a polynomial $\rho(z)$ (ρ, ϕ, z = cylindrical coordinates) for parametrizing the nuclear surface and a Saxon-Woods potential of the same con-

tour. Nilsson *et al.* [10]) and Krappe [11]) describe the deformed potential by adding higher multipoles to the ordinary Nilsson potential†. Nix *et al.* [12]) determine the shell-model potential which should correspond to a nuclear droplet of given shape on the basis of an effective nucleon-nucleon interaction.

Demeur and Reidemeister [13]) and Mosel and Greiner *et al.* [14]) have calculated the single-particle energies in a two-center potential composed of two harmonic oscillators. These calculations show the gradual change of the level scheme as one goes from the original spherical potential of the fissioning nucleus to the final configuration of two separated fragments. The wave functions for such a potential were also given by Wong [15]). In these last-mentioned papers [13-15]) the shell-model calculation is not correlated with the LDM.

In this paper, we describe the average potential for a strongly deformed fissioning nucleus by two oscillator potentials focussed around the centres of the emerging fragments and smoothly joined by an inverted oscillator which is to describe the neck part of the dumb-bell shaped nucleus (see fig. 1 for the z-dependent part of the potential.) This potential has already been treated in ref. [13]) for the case of heavy ion scattering. We discuss the physical justification of this model in subsect. 4.3. In sect. 2 we present the theory: We define the specific droplet model to be used in subsect. 2.1 and shortly rephrase the computation of the shell correction in subsect. 2.3. The shell-model potential is discussed in subsect. 2.2, which is complemented by the appendices B and C where the explicit form of the basic wave functions and of the matrix elements of the generalized spin-orbit and l^2 term is presented. Details of the droplet model are given in appendix A and of the numerical procedure in appendix D. The input parameters are listed in sect. 3. Sect. 4 contains results on level schemes (subsect. 4.1) and potential landscapes (subsect. 4.2).

2. Theory

2.1. DROPLET MODEL

The shape of the nucleus at the saddle point, as calculated by Cohen and Swiatecki within the droplet model, can be approximated to a high degree of accuracy by two spheroids connected by a hyperboloidal or a spheroidal neck [16]). Assuming that this parametrization continues to provide a suitable description when shell effects are included, we restrict ourselves to this family of nuclear shapes. Using cylindrical coordinates (z-axis = axis of rotational symmetry) the nuclear surface is represented in the following form:

$$\rho^2 = a_1^2 \left[1 - \frac{(z+z_1)^2}{c_1^2} \right], \quad \text{for } z < -z_0, \tag{1a}$$

$$\rho^2 = a_1^2 \left[1 - \frac{(z-z_1)^2}{c_1^2} \right], \quad \text{for } z > z_0. \tag{1b}$$

† Work based on a deformed Nilsson potential with a Gaussian central barrier is in preparation, private communication from Th. Johannson.

In the central region $-z_0 < z < z_0$ we distinguish three possibilities:

$$\rho^2 = a_0^2 \left(1 + \frac{z^2}{c_0^2}\right), \qquad \text{hyperboloid for prefission shapes,}$$

$$\rho^2 = a_0^2 \left(1 - \frac{z^2}{c_0^2}\right), \qquad \text{ellipsoid for prefission shapes,} \tag{1c}$$

$$\rho^2 = -a_0^2 \left(1 - \frac{z^2}{c_0^2}\right), \qquad \text{hyperboloid for postfission shapes.}$$

The usual requirement of a shape independent nuclear volume and, in our case, also of a smooth surface at the joining points $z = \pm z_0$ leaves us with three independent parameters to describe a particular shape. Examples of these nuclear shapes are given in fig. 12.

We represent the deformation energy in the LDM as a sum of a surface (E_{surf}), a curvature (E_{curv}) and a Coulomb term (E_{Coul}):

$$E_{\text{LDM}} = E_{\text{surf}} + E_{\text{curv}} + E_{\text{Coul}}, \tag{2}$$

$$E_{\text{surf}} = \beta_0 A^{\frac{2}{3}} \left[1 - \beta_1 \left(\frac{N-Z}{A}\right)^2\right] (B_{\text{surf}}(s) - 1), \tag{3a}$$

$$E_{\text{curv}} = \gamma_0 A^{\frac{1}{3}} \left[1 - \beta_1 \left(\frac{N-Z}{A}\right)^2\right] (B_{\text{curv}}(s) - 1), \tag{3b}$$

$$E_{\text{Coul}} = \frac{3}{5} \frac{e^2}{r_0} \frac{Z^2}{A^{\frac{1}{3}}} (B_{\text{Coul}}(s) - 1), \tag{3c}$$

where s denotes a set of shape parameters. The values for the parameters β_0, β_1, γ_0 and r_0 are taken from the literature and are listed in sect. 3. Essentially they are obtained by fitting the experimental ground state masses. The quantities B_{surf}, B_{curv} and B_{Coul} are the surface area, the mean curvature and the Coulomb-energy divided by the corresponding quantities for the spherical nucleus:

$$B_{\text{surf}} = \frac{1}{4\pi r_0^2 A^{\frac{2}{3}}} \int dS, \tag{4a}$$

$$B_{\text{curv}} = \frac{1}{8\pi r_0 A^{\frac{1}{3}}} \int dS \left(\frac{1}{R_1} + \frac{1}{R_2}\right), \tag{4b}$$

$$B_{\text{Coul}} = \frac{5 r_0 A^{\frac{1}{3}}}{3 e^2 Z^2} \cdot \frac{1}{2} \int d\tau_1 \, d\tau_2 \frac{\rho(r_1)\rho(r_2)}{|r_1 - r_2|}, \tag{4c}$$

where R_1 and R_2 are the Gaussian radii of principal curvature, dS and $d\tau$ are the surface and volume elements and $\rho(r)$ is the charge density. Explicit formulae are given in appendix A.

2.2. POTENTIAL MODEL

As stated in the preceding section, we only consider nuclear shapes which are composed of two spheroids smoothly connected by a hyperboloid of revolution (or by another spheroid). We have to choose the single-particle potential in such a way that the average nuclear density, calculated within this shell model, decreases from its value in the interior to zero in a narrow vicinity of the LD surface. Physically, the most reasonable choice appears to be a Saxon-Woods potential the range of which is determined by the surface of the corresponding LD [ref. [9]]. We hope that a less realistic but simpler model consisting of two smoothly joined oscillators will produce quite similar results. This hope is based on the surprising success of the Nilsson model in describing the spins of the ground and first excited states of deformed nuclei and, last but not least, on the observation that Strutinski's shell correction only depends on the density of shell-model levels near the Fermi energy. We expect this quantity to be sufficiently well reproduced by our less realistic potential. The greater simplicity of our model should enable us to speed up the numerical determination of the potential landscape which is a point of considerable practical interest. We shall comment on some numerical details in appendix D and on the physical justification of our potential model in subsect. 4.3.

We choose the shell-model potential U_0 such that surfaces of constant potential are spheroids connected by a hyperboloid of revolution with the same centres, joining points and axis ratios as the corresponding LD shape. Using cylindrical coordinates (ρ, ϕ, z) with the z-axis as the symmetry axis this is achieved by the following potential:

$$U_0(\rho, z) = \tfrac{1}{2}m\omega_\perp^2\rho^2 + V(z), \tag{5a}$$

$$V(z) = \begin{cases} \tfrac{1}{2}m\omega_1^2(z+z_1)^2, & \text{for } z < -z_0 \text{ (region I)} \\ \pm(V_0 - \tfrac{1}{2}m\omega_0^2 z^2), & \text{for } -z_0 < z < z_0 \text{ (region II)} \\ \tfrac{1}{2}m\omega_1^2(z-z_1)^2, & \text{for } z > z_0 \text{ (region III).} \end{cases} \tag{5b}$$

In eqs. (5b), (6a) and (6b) the upper sign holds for a hyperboloidal $(z_1 > z_0)$, the lower signs for a spheroidal $(z_1 < z_0)$ central part. The parameters are self-explanatory: m is the nucleon mass, $\omega_\perp$ is the oscillator frequency perpendicular to the axis of rotational symmetry, the parameters ω_1, ω_0 and V_0 describe the two-center potential in the z-direction. The requirement of smooth joining at $z = \pm z_0$ leads to the following relations:

$$\tfrac{1}{2}m\omega_1^2(z_0 - z_1)^2 = \pm(V_0 - \tfrac{1}{2}m\omega_0^2 z_0^2), \tag{6a}$$

$$\omega_1^2(z_0 - z_1) = \mp \omega_0^2 z_0. \tag{6b}$$

We assume in this section that all the potential parameters are known. We shall show in subsect. 2.3 how they are determined from a given shape of the droplet surface.

The eigenfunctions $\overset{\circ}{\psi}_\nu$ of the unperturbed Hamiltonian H_0

$$H_0 \overset{\circ}{\psi}_\nu = [T + U_0] \overset{\circ}{\psi}_\nu = \overset{\circ}{\varepsilon}_\nu \overset{\circ}{\psi}_\nu, \tag{7}$$

can be represented analytically; the corresponding eigenvalues $\overset{\circ}{\varepsilon}_\nu$ are obtained as solutions of a transcendental equation (see appendix B).

The potential $U_0(\rho, z)$ is not a realistic nuclear shell-model potential because it contains no spin-orbit term. Furthermore, a corrective term should be added which makes the eigenvalues of the potential more similar to the ones of a Saxon-Woods well. In the case of the Nilsson potential, the deformed harmonic oscillator is corrected by the term

$$V_{\text{corr}}^{N} = -\hbar \overset{\circ}{\omega}_0 \kappa \{ l_t \sigma + \mu (l_t^2 - \tfrac{1}{2} N(N+3)) \}. \tag{8}$$

Here the parameters κ and μ are chosen so as to reproduce the sequence of low-energy levels of odd-even nuclei as well as possible; $\overset{\circ}{\omega}_0$ is the oscillator frequency for the spherical nucleus, and l, σ are the operators of orbital angular momentum (times $1/\hbar$ and $2/\hbar$ times) the intrinsic spin. In Nilsson's ansatz for the potential, the orbital angular momentum l_t is formulated in terms of stretched coordinates x_t, y_t, z_t [ref. [10]] [†]. The corrective potential V_{corr}^{N} is diagonalized in the space of eigenfunctions of the Hamiltonian $[-\Delta(\rho_t, \theta_t, \phi_t) + \rho_t^2]$ where ρ_t, θ_t, ϕ_t are the polar coordinates corresponding to x_t, y_t, z_t and Δ is the Laplacian written in these coordinates. These basis functions can be characterized by the principal quantum number N. The expression $\tfrac{1}{2}N(N+3)$ in eq. (8) is the trace of the operator l_t^2 in the subspace defined by the principal quantum number N.

We wish to introduce a correction term of a similar structure with the difference that the more the orbitals are concentrated around the centres of the left- and right-hand spheroid, i.e. the more the two fragments are preformed, the more the orbital angular momentum is to be related not to the origin $z = 0$ but to the fragment centres at $z = \pm z_1$. This is achieved if we replace the position vector in the definition of l by a quantity proportional to ∇U_0:

$$l = r \times p \rightarrow (\nabla U_0 \times p) \text{ const.}$$

We also have to find a suitable generalization of the trace term $\tfrac{1}{2}N(N+3)$ which should be meaningful independently of the existence of the quantum number N and which should be equal to $\tfrac{1}{2}N(N+3)$ in the limit of the original spherical nucleus and the limit of two totally separated spherical nuclei. For this we write N as a function

---

[†] The coordinates are defined as

$$x_t = x \sqrt{\frac{m\omega_\perp}{\hbar}} ; \quad y_t = y \sqrt{\frac{m\omega_\perp}{\hbar}} ; \quad z_t = z \sqrt{\frac{m\omega_z}{\hbar}} ,$$

where ω_z is the oscillator frequency in the direction of the symmetry axis ($\equiv z$-axis).

of the eigenenergy e_N of an isotropic harmonic oscillator of frequency $\tilde{\omega}$

$$N = \frac{e_N}{\hbar\tilde{\omega}} - \frac{3}{2}, \tag{9a}$$

which leads to

$$\tfrac{1}{2}N(N+3) = \frac{1}{2}\left\{\left(\frac{e_N}{\hbar\tilde{\omega}}\right)^2 - \frac{9}{4}\right\}.$$

This expression can be made independent of the existence of the quantum number N, if we replace e_N by the eigenenergies $\overset{\circ}{\varepsilon}_\nu$ of the unperturbed Hamiltonian H_0.

$$N \rightarrow \frac{\overset{\circ}{\varepsilon}_\nu}{\hbar\tilde{\omega}} - \frac{3}{2}. \tag{9b}$$

The frequency $\tilde{\omega}$ must be weakly form-dependent in such a way that it becomes equal to the frequency $\tilde{\omega}_0$ for the original spherical nucleus and equal to the frequencies of the two emerging fragments in the case of totally separated oscillators. This can be achieved by the ansatz

$$\tilde{\omega} = \tilde{\omega}_0 \sqrt{B_{\mathrm{curv}}(s)}, \tag{10}$$

where $B_{\mathrm{curv}}(s)$ is the ratio of the mean curvatures of the deformed and spherical nucleus:

$$B_{\mathrm{curv}}(s) = \frac{\displaystyle\int_{\mathrm{deformed\,shape}} dS \left(\frac{1}{R_1} + \frac{1}{R_2}\right)}{\displaystyle\int_{\mathrm{spherical\,shape}} dS \left(\frac{1}{R_1} + \frac{1}{R_2}\right)}. \tag{11}$$

The shape dependence of $B_{\mathrm{curv}}(s)$ is very smooth as it should be. The only motivation of this choice is that it exhibits the desired behaviour in the limiting cases and that it smoothly interpolates between them.

We thus arrive at the following form of the corrective operator V_{corr}:

$$V_{\mathrm{corr}} = -\frac{\tilde{\omega}}{\hbar}\kappa\left\{\frac{\hbar}{m\tilde{\omega}^2}\sigma(\nabla U_0 \times p) + \mu\frac{(\nabla U_0 \times p)^2}{(m\tilde{\omega}^2)^2} - \tfrac{1}{2}\mu\hbar^2\left[\left(\frac{\overset{\circ}{\varepsilon}_\nu}{\hbar\tilde{\omega}}\right)^2 - \frac{9}{4}\right]\right\}. \tag{12}$$

If the potential U_0 is a spherical oscillator ($U_0 = \tfrac{1}{2}m\tilde{\omega}_0^2 r^2$), the form (12) of V_{corr} becomes identical to the form (8) used by Nilsson. If the potential U_0 consists of two totally separated spherical oscillators, the potential V_{corr} is effectively equal to the Nilsson term (8) for each of the two oscillators. The generalized form of the spin-orbit and l^2 terms are the simplest scalar operators which can be constructed from the vectors σ, p and ∇U_0. The choice of these terms is thus directly motivated. On the other hand, the generalization (12) of the trace term $\tfrac{1}{2}N(N+3)$ seems to be rather arbitrary. In this context, two remarks are in order: (i) The Strutinski shell correction

depends only on *differences* between discrete single-particle levels and averages of single-particle energies. Therefore, the influence of the trace term on the potential landscape is not large in any case. (ii) The motivation of adding a trace term is just to make the level schemes calculated on the basis of (12) agree with Nilsson's choice in the case of a spherical nucleus and two completely separated spherical fragments. This has the advantage that one may use the same or nearly the same values of κ and μ which were adjusted by Nilsson [10]) and other authors [9]) to obtain a correct level sequence for odd nuclei.

A correct level sequence can only be achieved if the value of κ depends gently on the principal quantum number N [refs. [8,10])], i.e. κ must be chosen weakly state dependent.

Seeger and Perisho [8]) showed that an empirically successful choice of this state dependence is given by

$$\kappa = \kappa_N = \frac{\kappa_0}{\sqrt[3]{\frac{1}{2}(N+1)(N+2)}}. \tag{13}$$

Again, we generalize this form by replacing N according to (9b) which leads to

$$\kappa = \frac{2\kappa_0}{\sqrt[3]{(2\mathring{\varepsilon}_v/\hbar\tilde{\omega})^2 - 1}}.$$

The operator V_{corr} defined in eq. (12) has non-diagonal elements in the basis of the eigenfunctions $\mathring{\psi}_v$ of H_0. So we replace $\mathring{\varepsilon}_v$ by the arithmetic mean of the eigenenergies $\mathring{\varepsilon}_{v_1}, \mathring{\varepsilon}_{v_2}$ corresponding to the bra and ket state:

$$\kappa = \frac{2\kappa_0}{\sqrt[3]{[(\mathring{\varepsilon}_{v_1} + \mathring{\varepsilon}_{v_2})/\hbar\tilde{\omega}]^2 - 1}}, \tag{14}$$

in the matrix element $\langle \mathring{\psi}_{v_1} | V_{\text{corr}} | \mathring{\psi}_{v_2} \rangle$.

We emphasize that this choice of κ represents an arbitrary generalization of a form of κ which had turned out to be empirically successful. Whether this generalization is useful or not can only be decided by comparing the calculated level scheme for strongly deformed nuclei (e.g. in the second minimum) with experimental evidence.

It is this arbitrariness in the detailed form of V_{corr} which is a rather strong argument in favour of using a deformed Saxon-Woods potential as is done by the authors of ref. [9]). There, no l^2 term occurs and the spin-orbit constant is likely to be state- and shape-independent. On the other hand, both are phenomenological potentials in the first place, and furthermore the shell correction of Strutinski as a difference term is likely to be quite insensitive to finer details of the potential.

The corrective potential (12), (14) is diagonalized in a sufficiently large subspace of eigenfunctions $\mathring{\psi}_v$. We emphasize that the basis states $\mathring{\psi}_v$ already include the effect of an arbitrarily strong deformation within the admitted family of shapes. Consequently, the dimension of the space of basis functions need not be increased as we go from

small to large deformations like a strong constriction in the neck part. This is a rather important advantage which is gained through the simplicity of our potential model.

2.3. DEFORMATION ENERGY ACCORDING TO STRUTINSKI'S METHOD

We calculate the deformation energy according to the method of Strutinski [7]: The deformation energy is given as the sum of the LD part E_{LDM}, a correction due to the pairing, and a shell correction.

$$\mathscr{E} = E_{LDM} + (E_{BCS} - E_{SM}) + E_{SC}. \tag{15}$$

The pairing term is given by the difference between the BCS energy E_{BCS} and the sum E_{SM} of occupied single-particle energies [17,18].

$$E_{BCS} - E_{SM} = \varepsilon_{odd} + \sum_{v>0} 2v_v^2(\varepsilon_v - \tfrac{1}{2}G^n v_v^2)$$

$$- \frac{\varLambda^{n\,2}}{G^n} + \sum_{\mu>0}'' 2v_\mu^2(\varepsilon_\mu - \tfrac{1}{2}G^p v_\mu^2) - \frac{\varLambda^{p\,2}}{G^p} - \sum_v' \varepsilon_v - \sum_\mu' \varepsilon_\mu. \tag{16}$$

Here, G^n, $\varLambda^n$, v_v^2, G^p, $\varLambda^p$, v_μ^2 are the pairing force matrix element, the gap parameter and the occupation probability for neutrons and protons, respectively, Indices $v(\mu)$ indicate neutron (proton) quantities; $\sum''$ means that the single-particle energy ε_{odd} occupied by the unpaired proton is to be omitted from the summation; $\sum'$ means summation over states below the Fermi level only. A completely analogous equation holds for a system with an odd neutron number. In the case of a doubly even nucleus there is no term ε_{odd} and no exclusion in the second sum.

The shell correction E_{SC} is the difference between the sum of occupied single-particle energies and an average of this sum which is obtained on the basis of a smooth level distribution $g^n(\varepsilon)$, $g^p(\varepsilon)$ for neutrons and protons [7].

$$E_{SC} = E_{SM} - \int_{-\infty}^{\varLambda^n} d\varepsilon\, \varepsilon g^n(\varepsilon) - \int_{-\infty}^{\varLambda^p} d\varepsilon\, \varepsilon g^p(\varepsilon), \tag{17}$$

$$g^n(\varepsilon) = \frac{1}{\sqrt{\pi}\gamma} \sum_v \left[\frac{3}{2} - \left(\frac{\varepsilon - \varepsilon_v}{\gamma}\right)^2\right] e^{-((\varepsilon - \varepsilon_v)/\gamma)^2}, \tag{18}$$

where the upper limit of the integration is defined by

$$\int_{-\infty}^{\varLambda^n} d\varepsilon\, g^n(\varepsilon) = N. \tag{19}$$

Equations analogous to (18) and (19) hold for protons.

We still have to establish a one to one correspondence between the parameters specifying the shape of the LD and the ones defining the potential U_0 (see eqs. (5a) and (5b)]. For this we require that the surface of constant potential

$$U_0(\rho, z) = k_0 \tag{20}$$

coincides with the given surface of the LD. If the constant k_0 is known, we thereby uniquely specify the potential parameters. We determine k_0 by requiring that in the case of a spherical oscillator of frequency $\overset{\circ}{\omega}_0$ the surface defined by (9a) should be identical to the surface of a sphere with the LD radius $R = r_0 A^{\frac{1}{3}}$

$$\tfrac{1}{2} m \overset{\circ}{\omega}_0^2 R^2 = k_0. \tag{21}$$

The frequency $\overset{\circ}{\omega}_0$ is chosen differently for neutrons and protons; it is adjusted so as to approximate the experimental rms radius of the neutron and proton distribution.

We remark that, contrary to the Nilsson model, equipotential surfaces which do not coincide with the LD surface, generally do not enclose a volume independent of deformation.

3. Parameters of the theory

The LDM part of the deformation energy contains the radius parameter r_0, the surface constant β_0 and the curvature constant γ_0, and the parameter β_1 which determines the symmetry energy (see eqs. (2)ff.). We choose the same numerical values as v. Groote and Hilf [5]:

$$r_0 = 1.123 \text{ fm}, \qquad \beta_1 = 1.7826,$$
$$\beta_0 = 17.8 \text{ MeV}, \qquad \gamma_0 = 6.5 \text{ MeV}.$$

The shell-model part contains the well-known parameters κ and μ of the Nilsson model [13]. Here, we use the values given by Seeger and Perisho [8] in connection with the generalized state dependence of κ [eqs. (14)]

$$\kappa_0 = 0.18, \qquad \mu = 0.62 \quad \text{for protons,}$$
$$\kappa_0 = 0.21, \qquad \mu = 0.308 \quad \text{for neutrons.}$$

The oscillator energy unit $\hbar \overset{\circ}{\omega}_0$ is taken to be

$$\hbar \overset{\circ}{\omega}_0 = 38/A^{\frac{1}{3}} \text{ MeV, for protons,}$$
$$\hbar \overset{\circ}{\omega}_0 = 44/A^{\frac{1}{3}} \text{ MeV, for neutrons.}$$

The pairing force constants were taken over from ref. [18]. They are fitted to the observed odd-even mass differences of nuclei in the actinide region

$$G^n = 17/A \text{ MeV}; \qquad G^p = 20.5/A \text{ MeV}.$$

The parameter γ for the level density formula (18) was taken to be

$$\gamma = 5 \text{ MeV}$$

which is approximately $0.7 \hbar \overset{\circ}{\omega}_0$ for nuclei in the actinide region.

4. Results

4.1. SINGLE-PARTICLE ENERGY SCHEMES

In this section, we show the migration of single-particle levels as a function of half the distance between the centres of the two fragments (z_1). As the two remaining independent shape parameters, we choose the ratio a_1/c_1 of the half-axes of the left and right spheroid and the ratio a_0/c_0 of the half-axes of the central hyperboloid. The values for these parameters are fixed in the following way:

(i) The quantity a_1/c_1 is put equal to 1, which means that the spheroids in regions I and III [eq. (5b)] are spheres.

(ii) In the case of fig. 4, the ratio a_0/c_0 is also put equal to 1, while in figs. 2 and 3 this quantity is put equal to 1000 for prefission shapes [eq. (1c)]. The choice of this large value is equivalent to a model of two overlapping spheres, i.e. two oscillators without a region II. For postfission shapes, the joining point z_0, obtained for given values of z_1 and a_0/c_0, does not always correspond to a real value of the radial coordinate

$$\rho = \sqrt{-a_0^2 + a_0^2 z_0^2/c_0^2}.$$

In this case, we choose the ratio a_0/c_0 in such a way, that the hyperboloid touches the spheres at the points $\rho = 0$ and $z_0 = \pm(z_1 - c_1)$. With this choice of the shape parameters of the droplet, the parameters of the potential U_0 are uniquely specified.

In fig. 2 we show the spectrum of the unperturbed energy levels $\mathring{\varepsilon}_\nu$ [see eq. (7)]. For the limiting cases of the original spherical nucleus and the two completely separated spherical fragments, we may characterize these levels by the principal quantum number N. The central barrier for the largest value of z_1 shown in the diagram turns out to be $V_0 = 38.3$ MeV. The degeneracy which corresponds to completely separated spherical oscillators is only achieved for levels well below this value of V_0, as can be seen from the diagram.

In figs. 3 and 4, we show the level plot for the eigenvalues ε_ν of the complete Hamiltonian $H = H_0 + V_{corr}$. As to be expected, the level diagram is drastically changed by the spin-orbit coupling and the generalized l^2 correction. The intervals between corresponding energy levels should be larger by a factor of $2^{\frac{1}{3}}$ for the totally separated spherical oscillators as compared to the original potential, because the energy unit is known to be proportional to $A^{-\frac{1}{3}}$. This requirement is automatically fulfilled by our choice of V_{corr} and the conservation of potential volumes (see subsects. 2.2 and 2.3).

4.2. POTENTIAL LANDSCAPES

In this section, we present results for the deformation energy as calculated in the pure LDM [E_{LDM}, eq. (2)] and the LD model with shell and pairing corrections ($\mathscr{E}$, eq. (15)]. As independent shape parameters we use the ratios a_1/c_1, a_0/a_1 and a_0/c_0. In all calculations of potential surfaces the ratio a_0/c_0 is kept constant.

The potential surfaces are presented in the form of perspective views: The energy is
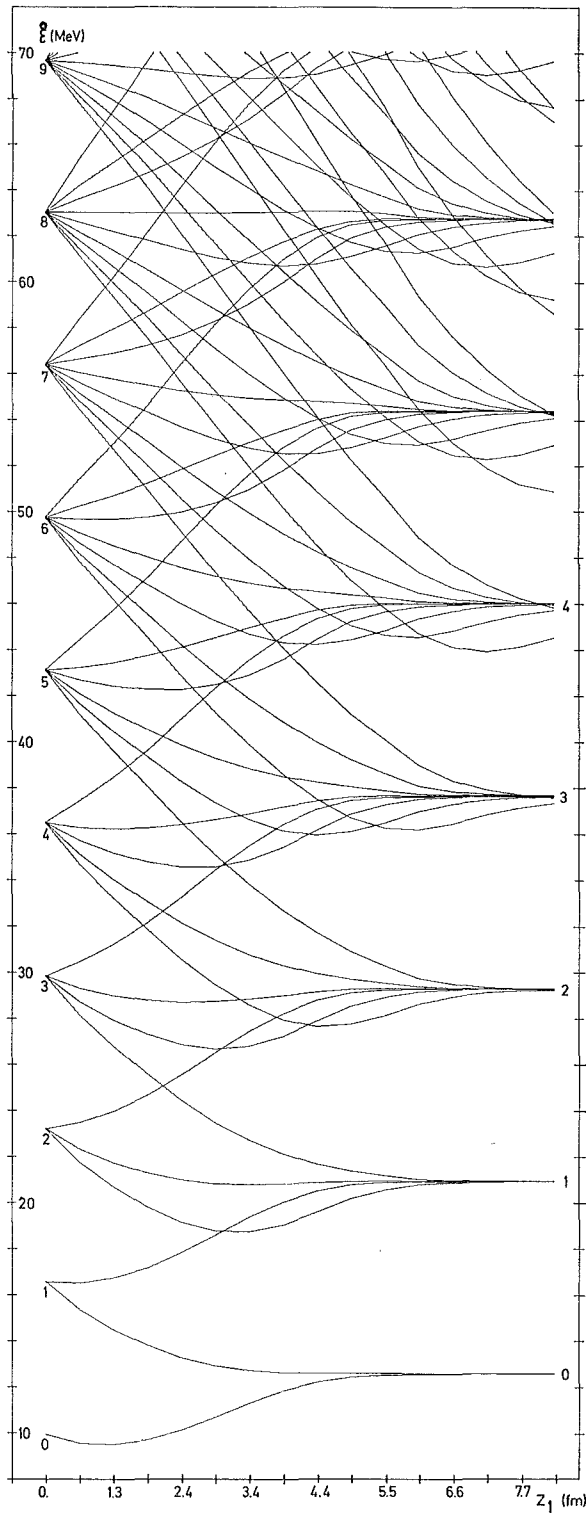
Fig. 2. Eigenenergies $\overset{\circ}{\varepsilon}$ of the unperturbed Hamiltonian H_0 as functions of the shape parameter z_1.
Parameters $a_1/c_1 = 1$, $a_0/c_0 = 1000$. Further information is given in subsect. 4.1.
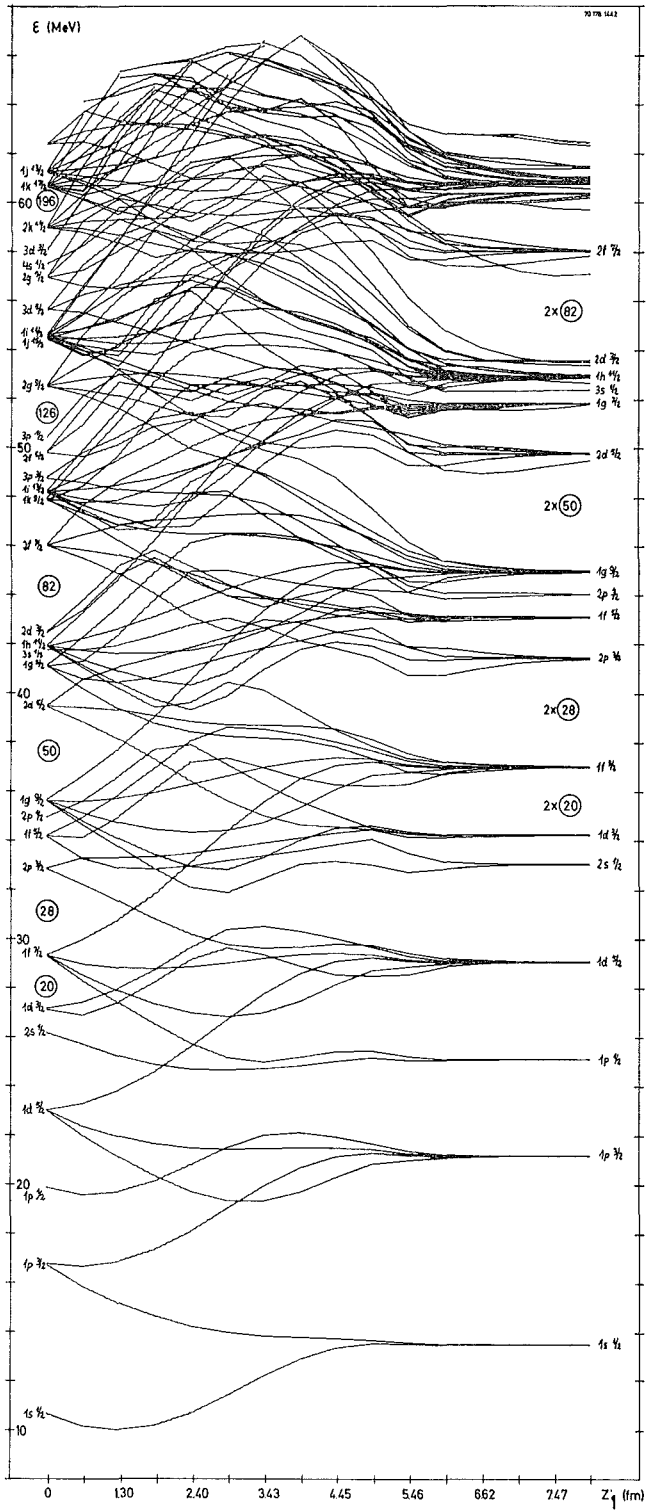
Fig. 3. Eigenenergies ε of the Hamiltonian H as functions of the shape parameter z_1. Parameters $a_1/c_1 = 1$, $a_0/c_0 = 1000$. Further information is given in subsect. 4.1.

Fig. 4. Same as fig. 3 but with the parameter $a_0/c_0 = 1$.

plotted on a vertical axis as a function of two shape parameters. The surfaces are seen from a direction perpendicular to this vertical axis, more specifically, the point of sight is chosen to be in the plane of zero energy and far away from the depicted part of the surface in order to avoid perspective distortions. This is schematically indicated in fig. 5. For every line drawn in figs. 6 to 11 one of the shape parameters a_1/c_1 or
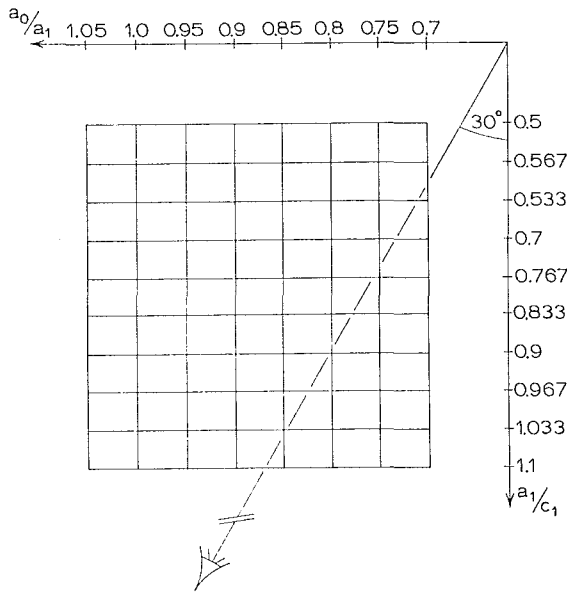
Fig. 5. Range of the variables a_1/c_1 and a_0/a_1 and angle of the point of sight for figs. 6 to 11. The deformation energy presented in figs. 6 to 11 is calculated for the crossing points of the lines of constant parameter a_1/c_1 and a_0/a_1. These straight lines are the projection into the plane of zero energy of the curves shown in figs. 6 to 11.

a_0/a_1 is kept constant. The projection of such curves on the plane of zero energy is shown in fig. 5. The deformation energy was calculated for the 80 crossing points in fig. 5. In the pictures of potential landscapes (figs. 6 to 11), the intervals between the lines connecting calculated points of the potential energy were subdivided into five equal parts. The energy at the crossing points of these additional lines is obtained by interpolation. By this way, it is made more obvious that the parameter lines form a surface.

A comparison of figs. 6 and 7 shows that the energy surface is drastically changed by the shell and pairing corrections. Fig. 7 shows a deformed ground state for ^{236}U (see table 1b). A second minimum of the function $\mathscr{E}$ is only slightly indicated in fig. 7 and becomes more pronounced if the energy is minimized with respect to all three independent shape parameters (compare tables 1b and 1d).

The saddle point of the LD energy is clearly seen in fig. 6. The corresponding values of the energy and shape parameters are given in table 1a. In fig. 7 we see two saddle
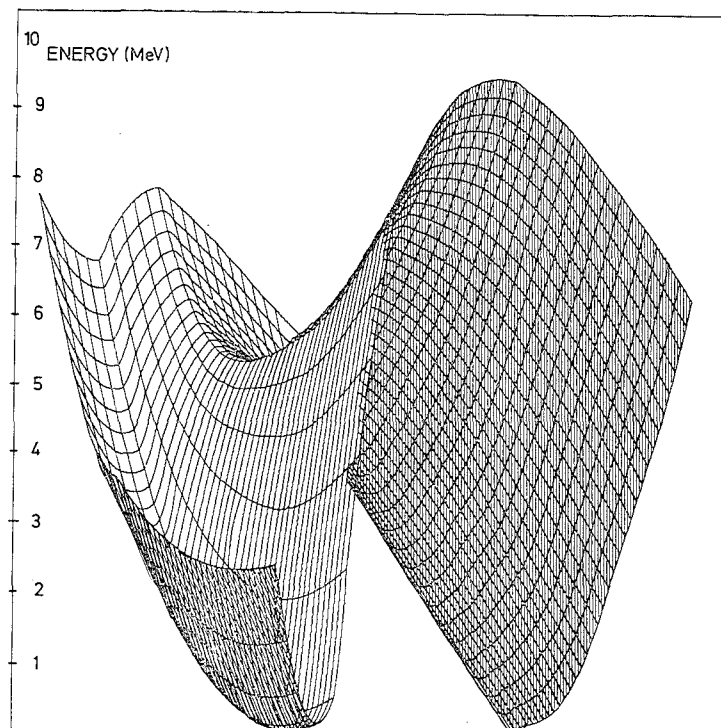
Fig. 6. Energy E_{LDM} of the liquid drop for the nucleus ^{236}U. The shape parameters a_1/c_1 and a_0/a_1 are varied in the range shown in fig. 5. The third shape parameter a_0/c_0 is given the constant·value $a_0/c_0 = 0.6$.
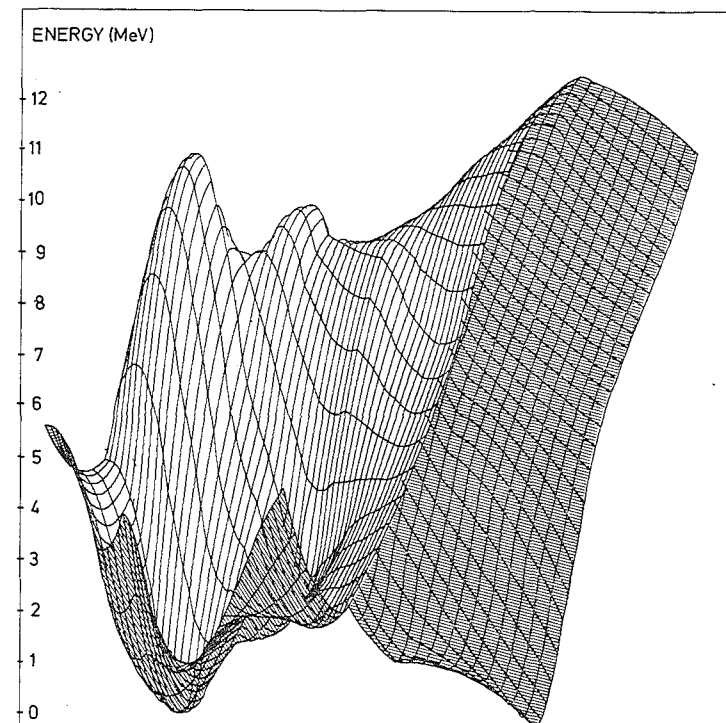
Fig. 7. Deformation energy $\mathscr{E}$ for ^{236}U. The ground state energy is normalized to zero. Parameter $a_0/c_0 = 0.6$.
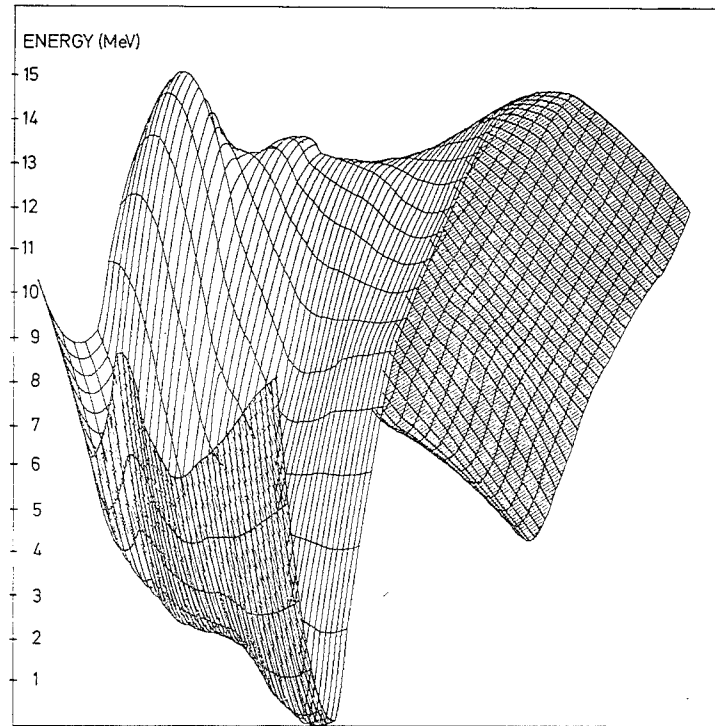
Fig. 8. Same as fig. 7, but with the following values of the constant pairing force $G^n = 20.5$ MeV$/A$, $G^p = 23.5$ MeV$/A$.
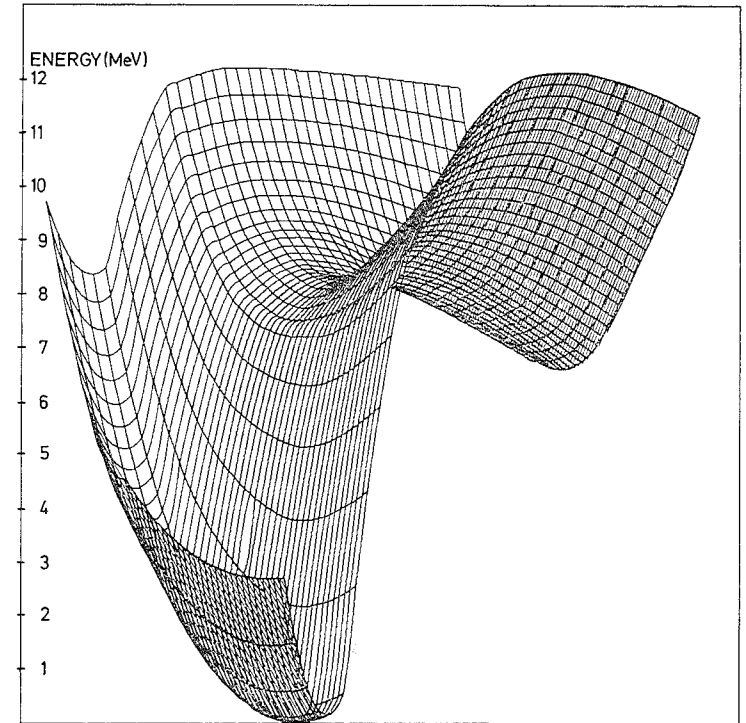
Fig. 9. Energy E_{LDM} of the liquid drop for ^{226}Ra. Parameter $a_0/c_0 = 0.6$.
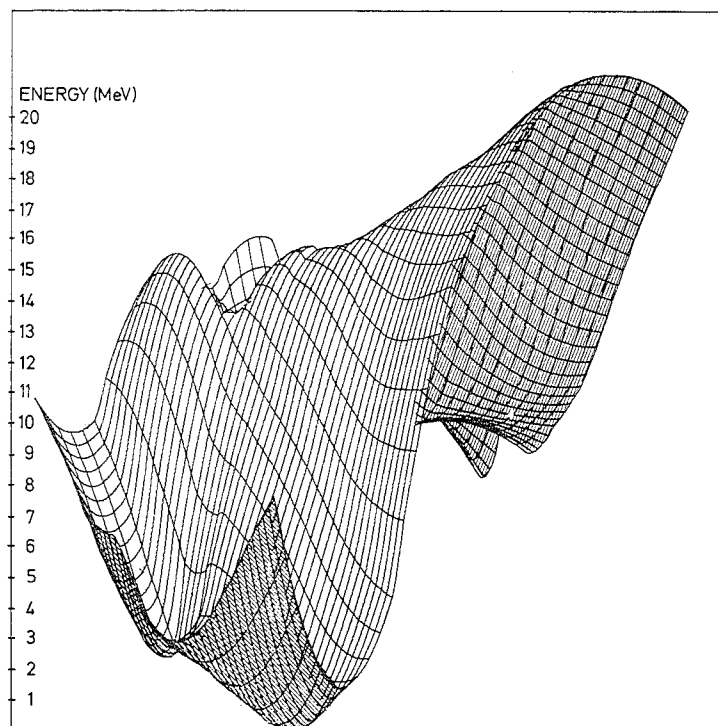
Fig. 10. Deformation energy $\mathscr{E}$ for ^{220}Ra. Parameter $a_0/c_0 = 0.6$.
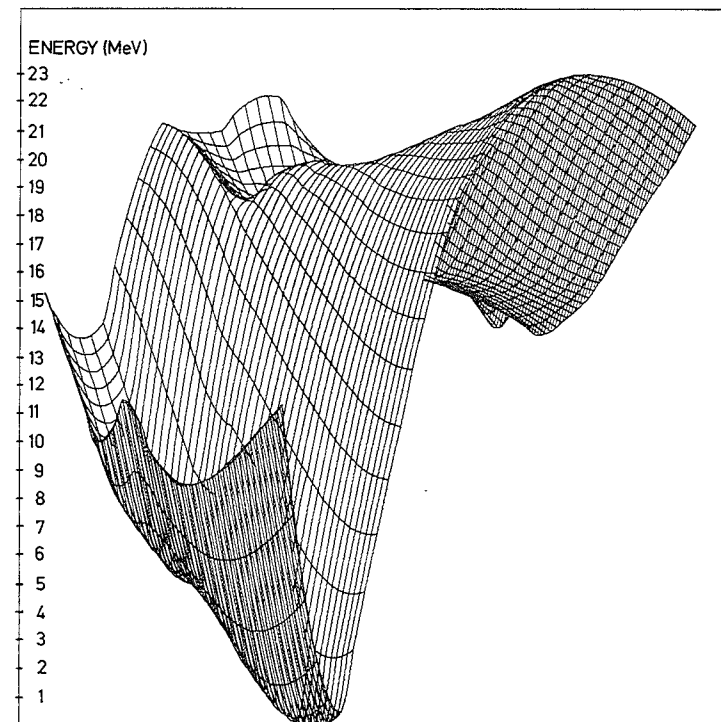
Fig. 11. Same as fig. 10 but with pairing force as in fig. 8.

TABLE 1

Minima and saddle points of the energy of deformation

1a) LDM saddle points for $a_0/c_0 = 0.6$

Nucleus	a_1/c_1	a_1/a_0	z_1	z_0	c_1	E_{LDM}
^{236}U	0.70	0.95	3.551	2.047	7.401	5.36
^{226}Ra	0.767	0.85	5.459	3.386	6.387	8.44

1b) Minima of the energy of deformation for $a_0/c_0 = 0.6$

Nucleus	a_1/c_1	a_0/a_1	z_1	z_0	c_1	$\mathscr{E}$
^{236}U	0.7	1	0	0	8.79	0
^{236}U	1.03	1	0	0	6.78	1.56
^{226}Ra	1.007	1	0	0	6.84	0
^{226}Ra	0.7	1	0	0	8.66	2.83

1c Saddle points for $a_0/c_0 = 0.6$

Nucleus	a_1/c_1	a_0/a_1	z_1	z_0	c_1	$\mathscr{E}$	Comment
^{236}U	0.83	0.90	4.64	3.06	6.22	9.24	see fig. 12c
^{236}U	0.69	0.94	3.81	2.16	7.43	9.0	
^{226}Ra	0.63	0.85	5.65	2.98	7.38	13.5	

1d Minima of the energy of deformation for ^{236}U with no restrictions on the shape parameters a_0/c_0

a_1/c_1	a_0/a_1	a_0/c_0	z_1	z_0	c_1	$\mathscr{E}$	Comment
0.7468	1.0038	0.5524	0.721	1.411	8.083	−0.25	see fig. 12a
0.85	0.9949	0.4521	1.509	1.176	7.052	−0.07	see fig. 12b

The energy of the lowest minimum (ground state) is normalized to zero. The unit of length is 1 fm, the unit of energy is 1 MeV.

points of comparable energy leading to fission (see also table 1c). The shape corresponding to one of them (smaller value of a_0/a_1) is plotted in fig. 12c. In all these results, the parameter a_0/c_0 was kept constant. We have used a search program to find minima of the deformation energy $\mathscr{E}$ as a function of the three shape parameters a_1/c_1, a_0/a_1 and a_0/c_0. Thus the ratio a_0/c_0 which so far had the fixed value of $a_0/c_0 = 0.6$ was now free to vary. The results are presented in table 1d, figs. 12a and 12b. The energy of the ground state relative to the LDM energy did not change very much compared to the results discussed before, however, the energy of the second minimum was appreciably lowered. This shows that in our parametrization, it is not possible to describe the relevant symmetric shapes with only two parameters. Recently it has been shown[†] that the saddle point energy for ^{236}U is lowered if asymmetric shapes are included.

† Private communications from S. G. Nilsson and V. M. Strutinski.

We have also performed calculations for the nucleus ^{226}Ra. Comparing these results with the ^{236}U data the following points are noteworthy: (i) The LDM-saddle point for radium is higher in energy and corresponds to a more constricted shape (fig. 9, table 1a); (ii) The energy $\mathscr{E}$ has two minima, as also found for uranium. The deepest minimum for radium corresponds to an almost spherical spheroid, the second
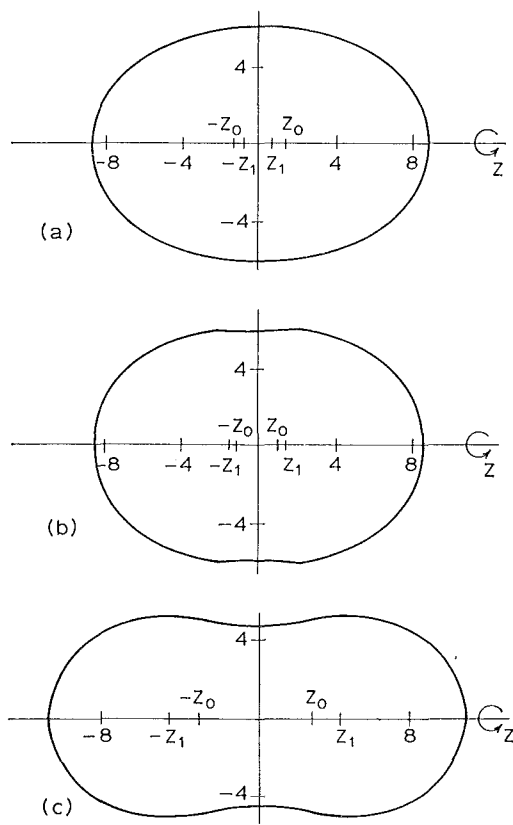
Fig. 12. Shapes for ^{236}U. The shape parameters are given in tables 1d and 1c.

minimum to a more prolate one (fig. 10, table 1b). Fig. 10 shows one saddle point leading to fission. Beyond this saddle point there appear to be *two* valleys. It would be interesting to find out whether both of them lead to an exit to fission. It is conceivable that once the asymmetric degree of freedom is included, one valley leads to symmetric and the other valley to asymmetric fission. This could thus provide an understanding of the three-peak mass distribution observed for fission of ^{226}Ra.

For a critical judgment of the results, so far presented, it is important to know how sensitive they are with respect to variations of the input parameters (sect. 3). For this,

we have arbitrarily enlarged the pairing force matrix elements. Using the values

$$G^n = 20.5/A \text{ MeV}, \qquad G^p = 23.5/A \text{ MeV},$$

we obtain the energy surfaces shown in figs. 8 and 11. These figures must be compared to figs. 7 and 10. The most striking difference is that, in the calculation with the enlarged pairing force, we obtain a minimum only for spherical shapes of the nuclei ^{236}U and ^{226}Ra. For prolate spheroidal shapes a steady increase of the energy is observed. This result is easily understood by noticing that the shell correction term to the LDM energy favours those nuclear shapes for which the level density at the Fermi surface is low, while the pairing interaction favours a high level density at the Fermi surface. For a nucleus like ^{236}U or ^{226}Ra the level density in question has a maximum for a spherical shape. If the pairing force matrix elements have a large value, there will only be one minimum of the deformation energy, since both the LDM and the pairing force term favour the spherical shape.

4.3. DISCUSSION

One wants to construct a potential form sufficiently general to describe the nucleus in all stages of the fission process up to the final separation of fragments. If, at the same time, one likes to retain oscillator potentials in view of their simplicity, one is automatically led to consider a two-center potential of the type which is proposed by us and several other authors [13−15]. We have stated already in subsect. 2.2 that the generalization of the correction terms (spin-orbit and l^2) involve some arbitrariness which does not appear if one uses a deformed Saxon-Woods potential. This arbitrariness however, concerns only finer details of the potential landscape which are anyhow probably beyond the scope of a phenomenological theory.

On the other hand, there is a more serious principal objection to the potential model we propose: In our potential model a barrier is introduced between the nascent fragments which is larger, the larger the central constriction of the nuclear droplet. Although it is quite obvious that a potential barrier must finally develop between the two separating parts, we would expect that, as a consequence of nuclear saturation, the potential barrier develops only in a rather *late* stage of the fission process, when the diameter of the neck part approaches twice the surface thickness (i.e. 2–4 fm). In our case, a sizeable barrier may already be present at the second saddle point ($V_0 = 5.6$ MeV for ^{236}U; $V_0 \approx 7$ MeV for ^{226}Ra). This barrier produces a reduced average density in the neck part while in fact there should be essentially the same average density in the neck and in the nascent fragments.

The answer to this criticism is that, in the Strutinski method, it is not the *average* density but the *fluctuation* of the density around the average droplet value which is to be determined by the potential model. While it is true that our potential model leads to an incorrect average density in the neck part, it may well reproduce the fluctuation correctly.

The fluctuation of the density is correlated with a fluctuation of the density of

single-particle levels near the Fermi-energy ε_F. It is this fluctuation of the level density which enters our calculation in terms of the shell correction. In a more realistic potential like the deformed Saxon-Woods potential, the main effect on the levels near ε_F of a constriction in the central part is that those single-particle levels are pushed upwards in energy which correspond to orbitals exhibiting in the neck part large amplitudes in ρ-direction.

In the two-center oscillator model we describe a central constriction by a barrier in the z-direction between the later fragments. The introduction of such a barrier will most strongly affect the single-particle states with the lowest number of nodes n_z in the z-direction: The corresponding energy $\overset{\circ}{\varepsilon}{}^z_{n_z}$ increases as a consequence of introducing the barrier. The total single-particle energy[†] $\overset{\circ}{\varepsilon}_\nu$ is the sum of the energy $\varepsilon^z_{n_z}$ in the z-direction and the energy $\overset{\circ}{\varepsilon}_{n_\perp A}$ in ρ-direction (see appendix A)

$$\overset{\circ}{\varepsilon}_\nu = \overset{\circ}{\varepsilon}{}^z_{n_y} + \overset{\circ}{\varepsilon}_{n_\perp A}.$$

For a state with low n_z to be near the Fermi energy ε_F, the energy $\overset{\circ}{\varepsilon}_{n_\perp A}$ must be large, i.e. the number $n_\perp$ of radial nodes ($\varepsilon_{n_\perp A} = \hbar\omega_\perp(n_\perp+1)$) must be *large*.

So we see that the main effect, in the vicinity of the Fermi energy, of introducing a barrier is to raise the single-particle energies corresponding to states with a higher number of radial nodes and a low number n_z of axial nodes. This is qualitatively the same effect as for the constricted Saxon-Woods potential. We, therefore, have reason to expect that the two-center potential reproduces correctly the effect *on the shell-correction* of a central constriction. Of course, the total density as well as the single-particle energies far below the Fermi energy are not meaningful quantities in this model.

Appendix A

EXPLICIT FORMULAE FOR THE DROPLET PART

Here we give formulae for the functions B_{surf}, B_{curv} and B_{Coul} i.e. the surface area, the mean curvature and the Coulomb energy divided by the corresponding quantities

[†] For the sake of simplicity, we base our discussion on the *unperturbed* eigenstates ν of H_0.

for the spherical nucleus. For the LD shape given by eqs. (1) the surface and curvature terms may be evaluated analytically

$$B_{surf} = \frac{1}{4\pi r_0^2 A^{\frac{2}{3}}} \int dS = \frac{1}{2r_0^2 A^{\frac{2}{3}}} \int dz \rho(z) \sqrt{1 + \left(\frac{d\rho}{dz}\right)^2} = \frac{1}{2r_0^2 A^{\frac{2}{3}}} I_s, \qquad (A.1)$$

$$B_{curv} = \frac{1}{8\pi r_0 A^{\frac{1}{3}}} \int dS \left(\frac{1}{R_1} + \frac{1}{R_2}\right)$$

$$= \frac{1}{4r_0 A^{\frac{1}{3}}} \int dz \left(1 - \frac{\rho(z)\dfrac{d^2\rho}{dz^2}}{1 + \left(\dfrac{d\rho}{dz}\right)^2}\right) = \frac{1}{4r_0 A^{\frac{1}{3}}} I_c. \qquad (A.2)$$

Using the function $\rho(z)$ given by eqs. (1) one obtains for the above integrals

$$I_s = \int dz \sqrt{\delta_1 + \delta_2 z^2} = \begin{cases} \frac{1}{2}z\sqrt{\delta_1 + \delta_2 z^2} + \dfrac{\delta_1}{2\sqrt{\delta_2}} \ln\left[\sqrt{\delta_2}\, z + \sqrt{\delta_1 + \delta_2 z^2}\right] \\ \qquad \text{for } \delta_2 > 0;\ \delta_1 + \delta_2 z^2 \geqq 0 \\[2mm] \frac{1}{2}z\sqrt{\delta_1 + \delta_2 z^2} + \dfrac{\delta_1}{\sqrt{-\delta_2}} \arcsin\left(\sqrt{\dfrac{-\delta_2}{\delta_1}}\, z\right) \\ \qquad \text{for } \delta_2 < 0;\ \delta_1 > 0;\ \delta_1 + \delta_2 z^2 \geqq 0 \quad (A.1a) \\[2mm] \sqrt{\delta_1}\, z \qquad \text{for } \delta_2 = 0;\ \delta_1 > 0 \end{cases}$$

$$I_c = \int \left(1 + \frac{\delta_3}{1 + \dfrac{\delta_2}{\delta_1} z^2}\right) dz = \begin{cases} z + \delta_3 \sqrt{\dfrac{\delta_1}{\delta_2}} \operatorname{arctg}\left(\sqrt{\dfrac{\delta_2}{\delta_1}}\, z\right) \quad \text{for } \dfrac{\delta_2}{\delta_1} > 0 \\[3mm] z + \delta_3 \sqrt{\dfrac{-\delta_1}{\delta_2}}\, \dfrac{1}{2} \ln\left(\dfrac{1 + \sqrt{\dfrac{-\delta_2}{\delta_1}}\, z}{1 - \sqrt{-\dfrac{\delta_2}{\delta_1}}\, z}\right) \quad \text{for } \dfrac{\delta_2}{\delta_1} < 0 \\[3mm] z(1 + \delta_3) \quad \text{for } \dfrac{\delta_2}{\delta_1} = 0. \qquad (A.2a) \end{cases}$$

The integration is extended over those values of z for which the function $\rho^2(z)$ is positive. The parameters δ_1, δ_2 and δ_3 depend on whether $\rho(z)$ is a spheroid or a hyperboloid:

$$\delta_1 = \begin{cases} a^2 & \text{for an ellipsoid} \\ a^2 & \text{for a hyperboloid for prefission shapes} \\ -a^2 & \text{for a hyperboloid for postfission shapes,} \end{cases}$$

$$\delta_2 = \begin{cases} -\dfrac{a^2}{c^2}\left(1-\dfrac{a^2}{c^2}\right) & \text{for an ellipsoid} \\[2mm] \dfrac{a^2}{c^2}\left(1+\dfrac{a^2}{c^2}\right) & \text{for both types of hyperboloids,} \end{cases}$$

$$\delta_3 = \begin{cases} \dfrac{a^2}{c^2} & \text{for an ellipsoid} \\[2mm] -\dfrac{a^2}{c^2} & \text{for both types of hyperboloids.} \end{cases}$$

The ratio B_{Coul} of the Coulomb energy of the deformed nucleus divided by the one of the spherical nucleus can be expressed in terms of a triple integral [20]).

$$B_{\text{Coul}} = \frac{1}{(r_0 A^{\frac{1}{3}})^5}\frac{15}{4}$$

$$\times \int_0^{2z_0} dz \int_0^1 dy \int_0^1 dw \; \frac{z F^2(z)F^2(yz)\sin^2(\pi w)}{2(1-y)+\sqrt{z^2(1-y)^2+F^2(z)+F^2(yz)-2F(z)F(yz)}\cos(\pi w)},$$

$$\text{(A.3)}$$

where $z_0 = (c_1+z_0)$, and $F(z) = \rho(z-z_0)$. We evaluate the integral in eq. (A. 3) numerically by means of a Gauss-Legendre quadrature formula with 32 support points for each of the three variables [†].

Appendix B

EIGENFUNCTIONS AND EIGEN-ENERGIES OF THE UNPERTURBED HAMILTONIAN H_0

In this appendix, we present the explicit form of the z-dependent part $\varphi_{n_z}(z)$ of the wave functions $\overset{\circ}{\psi}_\nu$ and of the secular equation. The results are very simply obtained and are also given in less detail in refs. [13-15]). If the Schrödinger equation (7) is written in cyclindrical coordinates (ρ, ϕ, z), it can be separated into three ordinary differential equations. The ρ- and ϕ-dependent part of the solution is trivial and will be given at the end of this section. The z-dependent part $\varphi_{n_z}(z)$ is a solution of the equation

$$\left[-\frac{\hbar^2}{2m}\partial_{zz}+V(z)\right]\varphi_{n_z}(z) = \overset{\circ}{\varepsilon}_{n_z}^z \varphi_{n_z}(z), \qquad \text{(B.1)}$$

where $V(z)$ is given by eq. (5b). In what follows, we omit the index n_z. If double signs appear, the upper and lower signs refer to central hyperboloid and central spheroid, respectively.

Introducing dimensionless variables in the different regions I, II, III [see eq. (5b)]

[†] We are grateful to Dr. Hasse for making a computer routine available to us which calculates the Coulomb energy using this method.

through the definitions ·

$$\xi = \alpha_1(z+z_1) = \sqrt{\frac{2m\omega_1}{\hbar}}(z+z_1),$$

$$\eta = \alpha_0 z = \sqrt{\frac{2m\omega_0}{\hbar}}\,z,$$

$$\zeta = \alpha_1(z-z_1),$$

$$a_1 = \frac{-\overset{\circ}{\varepsilon}{}^z}{\hbar\omega_1}\,;\quad a_0 = \pm\frac{V_0}{\hbar\omega_0} - \frac{\overset{\circ}{\varepsilon}{}^z}{\hbar\omega_0}\,,$$

we can write eq. (B. 1) as:

$$\partial_{\xi\xi}\varphi_{\mathrm{I}} - (\tfrac{1}{4}\xi^2 + a_1)\varphi_{\mathrm{I}} = 0,\tag{B.2}$$

$$\partial_{\eta\eta}\varphi_{\mathrm{II}} - (\mp\tfrac{1}{4}\eta^2 + a_0)\varphi_{\mathrm{II}} = 0,\tag{B.2a}$$

$$\partial_{\zeta\zeta}\varphi_{\mathrm{III}} - (\tfrac{1}{4}\zeta^2 + a_1)\varphi_{\mathrm{III}} = 0.\tag{B.2b}$$

Here, φ_{I}, φ_{II}, φ_{III} denote the wave function $\varphi(z)$ in the regions I, II and III.

We choose the functions $\mathscr{U}_1$ and $\mathscr{U}_2$, defined in eqs. (B.3), (B.3a) as linearly in-dependent basic solutions of the eqs. (B.2), (B.2b) and the lower sign case of eqs. (B.2a). In the case of the upper sign in eqs. (B.2a) (central neck), the differential equation differs from the remaining ones by the sign of one term. We then have to use as independent solutions of (B.2a) the functions $\mathscr{U}_3$, $\mathscr{U}_4$ defined in eqs. (B.4), (B.4') [see ref. [21])], chapter 19].

$$\mathscr{U}_1(a, v) = e^{-\tfrac{1}{4}v^2}\phi(\tfrac{1}{2}a+\tfrac{1}{4};\tfrac{1}{2};\tfrac{1}{2}v^2),\tag{B.3}$$

$$\mathscr{U}_2(a, v) = e^{-\tfrac{1}{4}v^2}v\phi(\tfrac{1}{2}a+\tfrac{3}{4};\tfrac{3}{2};\tfrac{1}{2}v^2),\tag{B.3a}$$

$$\mathscr{U}_3(a, v) = \mathscr{U}_1(-ia, i^{\frac{1}{2}}v),\tag{B.4}$$

$$\mathscr{U}_4(a, v) = \mathscr{U}_2(-ia, i^{\frac{1}{2}}v).\tag{B.4a}$$

Here, v stands for one of the dimensionless variables ξ, η, ζ and the parameter a for one of the dimensionless quantities a_0, a_1. The symbol ϕ denotes the confluent hyper-geometric function.

The functions $\mathscr{U}_1$, $\mathscr{U}_2$, $\mathscr{U}_3$, $\mathscr{U}_4$ are calculated from recursion relations (HMF 19.2.7, HMF 19.16.3). In region III (I) we have to choose as a solution a linear com-bination of $\mathscr{U}_1$ and $\mathscr{U}_2$ which tends to zero at large values of $v(-v)$. This solution is the parabolic cylinder function $U(a, v)$ defined by (see HMF 19.3.1):

$$U(a, v) = \cos\left[\pi(\tfrac{1}{4}+\tfrac{1}{2}a)\right]Y_1(a, v) - \sin\left[\pi(\tfrac{1}{4}+\tfrac{1}{2}a)\right]Y_2(a, v),\tag{B.6}$$

$$Y_1(a, v) = \frac{\Gamma(\tfrac{1}{4}-\tfrac{1}{2}a)}{\sqrt{\pi}2^{\tfrac{1}{2}a+\tfrac{1}{4}}}\mathscr{U}_1(a, v),\tag{B.6a}$$

$$Y_2(a, v) = \frac{\Gamma(\frac{3}{4} - \frac{1}{2}a)}{\sqrt{\pi}2^{\frac{1}{2}a - \frac{3}{4}}} \mathscr{Y}_2(a, v). \tag{B.6b}$$

As a consequence of the reflection symmetry of H_0, the eigenstates $\overset{\circ}{\psi}_\nu$ as well as the z-dependent parts are either "gerade" or "ungerade". This leads to the following form of the solution $\varphi(z)$:

"gerade "states:

$$\varphi_{\mathrm{I}} = A_{\mathrm{I}} \, U(a_1, -\xi),$$

$$\varphi_{\mathrm{II}} = \begin{cases} A_{\mathrm{II}} \, \mathscr{Y}_3(a_0, \eta) & \text{for } z_0 < z_1 \text{ (central hyperboloid)} \\ A_{\mathrm{II}} \, \mathscr{Y}_1(a_0, \eta) & \text{for } z_0 > z_1 \text{ (central spheroid)} \end{cases} \tag{B.7}$$

$$\varphi_{\mathrm{III}} = A_{\mathrm{I}} \, U(a_1, \zeta),$$

"ungerade" states:

$$\varphi_{\mathrm{I}} = A_{\mathrm{I}} \, U(a_1, -\xi),$$

$$\varphi_{\mathrm{II}} = \begin{cases} A_{\mathrm{II}} \, \mathscr{Y}_4(a_0, \eta) & \text{for } z_0 < z_1 \text{ (central hyperboloid)} \\ A_{\mathrm{II}} \, \mathscr{Y}_2(a_0, \eta) & \text{for } z_0 > z_1 \text{ (central spheroid)} \end{cases} \tag{B.7a}$$

$$\varphi_{\mathrm{III}} = -A_{\mathrm{I}} \, U(a_1, \zeta).$$

The requirement of continuity of $\varphi(z)$ and $d\varphi/dz$ at the joining points $z = \pm z_0$ determines the ratio $A_{\mathrm{I}}/A_{\mathrm{II}}$ and the eigenvalues $\mathring{\varepsilon}^z$:

$$\frac{A_{\mathrm{I}}}{A_{\mathrm{II}}} = \frac{\mathscr{Y}_\sigma(a_0, \eta_0)}{U(a_1, \zeta_0)}, \tag{B.8}$$

$$\alpha_1 \left[\frac{\partial}{\partial \zeta} \ln U(a_1, \zeta) \right]_{\zeta = \zeta_0} = \alpha_0 \left[\frac{\partial}{\partial \eta} \ln \mathscr{Y}_\sigma(a_0, \eta) \right]_{\eta = \eta_0}, \tag{B.9}$$

with $\zeta_0 = a_1(z_0 - z_1)$, $\eta_0 = \alpha_0 z_0$ and $\sigma = 1, 2, 3, 4$ according to the case considered [see eqs. (B.7), (B.7a)]. Through the normalization condition

$$1 = |A_{\mathrm{II}}|^2 \frac{2}{\alpha_0} \int_0^{\eta_0} d\eta \, \mathscr{Y}_\sigma^2(a_0, \eta) + |A_{\mathrm{I}}|^2 \frac{2}{\alpha_1} \int_{\zeta_0}^\infty d\zeta \, U^2(a, \zeta), \tag{B.10}$$

and eq. (B.8), A_{I} and A_{II} are defined up to an irrelevant common phase.

If the potential $V(z)$ consists of two oscillators only (no region II), the following simpler forms of the eigenvalue equation and normalization condition hold:

$$\left[\frac{\partial}{\partial \zeta} \ln U(a_1, \zeta) \right]_{\zeta = \zeta_0} = \left[\frac{\partial}{\partial \xi} \ln U(a_1, -\xi) \right]_{\xi = \xi_0}, \tag{B.9a}$$

$$1 = |A_{\mathrm{II}}|^2 \frac{2}{\alpha_1} \int_{\zeta_0}^\infty d\zeta \, U^2(a_1, \zeta). \tag{B.10a}$$

The eigenvalue eqs. (B.9) or (B.9a) must be solved numerically. This can be accomplished with a simple and very rapidly working computer programme.

The part $\chi(\rho, \phi)$ of $\overset{\circ}{\psi}_\nu$ which depends on ρ and ϕ is given by refs. [22,23])

$$\chi_{n_\perp \Lambda}(\rho, \phi) = \mathcal{N}(2\pi)^{-\frac{1}{2}} e^{i\Lambda\phi} e^{-\frac{1}{2}\alpha\rho^2} (\sqrt{\alpha}\rho)^\Lambda L_t^\Lambda(\alpha\rho^2), \tag{B.11}$$

where $\alpha = m\omega_\perp/\hbar$ and $t = \frac{1}{2}(n_\perp - \Lambda)$. The function L_t^Λ is the associated Laguerre polynomial[†]; t is the number of nodes in the direction perpendicular to the z-axis and Λ can have the values $\pm\Lambda = n_\perp, n_\perp - 2, n_\perp - 4, \ldots 1$ or 0. Here $\mathcal{N}$ is a normalization factor and the total basic state $\overset{\circ}{\psi}_\nu$ is the product of the wave functions considered

$$\overset{\circ}{\psi}_\nu(\rho, \phi, z) = \chi_{n_\perp \Lambda}(\rho, \phi)\varphi_{n_z}(z). \tag{B.12}$$

If the counting index $n_z = 0$ for the lowest "gerade" solution, n_z is equal to the number of nodes in z-direction.

Appendix C

MATRIX-ELEMENTS OF THE GENERALIZED l^2 AND SPIN-ORBIT TERM

We consider here in some detail the evaluation of matrix elements of the operator V_{corr} [eq. (12)] in the basis discussed in appendix B.

We define the two operators

$$V_1 = \frac{-\kappa}{m\tilde{\omega}}(\nabla U_0 \times p)\sigma = \gamma_1(\nabla U_0 \times p) \cdot \sigma, \tag{C.1}$$

$$V_2 = \frac{-\kappa\mu}{\hbar m^2 \tilde{\omega}^3}(\nabla U_0 \times p)^2 = \gamma_2(\nabla U_0 \times p)^2, \tag{C.2}$$

and the auxiliary vector C

$$C = \nabla U_0 \times p. \tag{C.3}$$

The spherical components of this vector are

$$C_\pm = \mp \frac{1}{\sqrt{2}}(C_x \pm iC_y)$$

$$= \mp i\left(m\omega_\perp^2 \rho \pm p_z - \frac{dV(z)}{dz} p_\pm\right), \tag{C.4}$$

$$C_0 = C_z = m\omega_\perp^2 l_z. \tag{C.5}$$

In the last equation, l_z is the component of angular momentum along the z-axis

$$l_z = (r \times p)_z.$$

[†] Note that

$$(L_p^k)_{\text{ref. 19}} = (-)^k(L_{p-k}^k)_{\text{our notation}}.$$

The spherical components $\sigma_\pm$, $\rho_\pm$ and $p_\pm$ are defined in an analogous way as $C_\pm$.

Using eqs. (C.4) and (C.5) it is found that V_1 and V_2 can be written in the following way:

$$V_1 = -\gamma_1 \left\{ -m\omega_\perp^2(\rho_-\,\sigma_+ + \rho_+\,\sigma_-)\frac{i}{\sqrt{2}}\,p_z \right.$$

$$\left. + \frac{dV(z)}{dz}\frac{i}{\sqrt{2}}(\sigma_-\,p_+ + \sigma_+\,p_-) - m\omega_\perp^2\,\sigma_z\,l_z \right\}, \quad (C.6)$$

$$V_2 = \gamma_2 \left\{ (m\omega_\perp^2)^2\rho^2 p_z^2 + \left(\frac{dV}{dz}\right)^2 p_\rho^2 \right.$$

$$\left. + m\omega_\perp^2 \left[(\rho_+\,p_- + \rho_-\,p_+)\left(p_z\frac{dV}{dz} + \frac{dV}{dz}\,p_z\right) + 2i\hbar\frac{dV}{dz}\,p_z \right] + (m\omega_\perp^2)^2 l_z^2 \right\}. \quad (C.7)$$

For deriving eq. (C.7) one uses the identities:

$$\rho_+\rho_- + \rho_-\rho_+ = -\rho^2 = -x^2 - y^2,$$

$$p_+p_- + p_-p_+ = -p_\rho^2 = -p_x^2 - p_y^2,$$

$$[\rho_+, p_-] = [\rho_-, p_+] = -i\hbar.$$

The advantage of expressing V_1 and V_2 in this way is that all operators acting on the variable ρ can be expressed simply in terms of creation and destruction operators for a two-dimensional harmonic oscillator [24]. They are defined by

$$A_\pm^\dagger = \frac{1}{\sqrt{2}}(a_x^\dagger \pm ia_y^\dagger),$$

$$a_i^\dagger|n_i\rangle = (n_i+1)^{\frac{1}{2}}|n_i+1\rangle, \qquad i = x, y.$$

We indicate for completeness the relations between these operators and those occurring in V_1 and V_2.

$$\rho_+ = -\left(\frac{\hbar}{2m\omega_\perp}\right)^{\frac{1}{2}}(A_+^\dagger + A_-),$$

$$\rho_- = \left(\frac{\hbar}{2m\omega_\perp}\right)^{\frac{1}{2}}(A_-^\dagger + A_+),$$

$$p_+ = i(\tfrac{1}{2}m\hbar\omega_\perp)^{\frac{1}{2}}(A_+^\dagger - A_-), \qquad (C.8)$$

$$p_- = i(\tfrac{1}{2}m\hbar\omega_\perp)^{\frac{1}{2}}(A_-^\dagger - A_+).$$

The non-zero matrix elements of these operators in the representation $|n_\perp\Lambda\rangle$ defined

in appendix B are

$$\langle n_\perp \pm 1, \Lambda \pm 1|\rho_\pm|n_\perp \Lambda\rangle = \mp \left(\frac{\hbar}{2m\omega_\perp}\right)^{\frac{1}{2}} \frac{1}{\sqrt{2}} (n_\perp + \Lambda + 1 \pm 1)^{\frac{1}{2}},$$

$$\langle n_\perp \mp 1, \Lambda \pm 1|\rho_\pm|n_\perp \Lambda\rangle = \mp \left(\frac{\hbar}{2m\omega_\perp}\right)^{\frac{1}{2}} \frac{1}{\sqrt{2}} (n_\perp - \Lambda + 1 \mp 1)^{\frac{1}{2}}, \qquad (C.9)$$

$$\langle n_\perp \pm 1, \Lambda \pm 1|p_\pm|n_\perp \Lambda\rangle = -i(\tfrac{1}{2}m\hbar\omega_\perp)^{\frac{1}{2}} \frac{1}{\sqrt{2}} (n_\perp + \Lambda + 1 \pm 1)^{\frac{1}{2}},$$

$$\langle n_\perp \mp 1, \Lambda \pm 1|p_\pm|n_\perp \Lambda\rangle = i(\tfrac{1}{2}m\hbar\omega_\perp)^{\frac{1}{2}} \frac{1}{\sqrt{2}} (n_\perp - \Lambda + 1 \mp 1)^{\frac{1}{2}}.$$

Thus the matrix elements of V_1 and V_2 can be calculated if the matrix elements of the z-dependent operators are known. Although the functions $\varphi_{n_z}(z)$ are "analytically" represented (see appendix B), the matrix elements of the z-dependent operators in eqs. (C.6) and (C.7) cannot be given in a simple closed form. They could be reduced to rather complicated expressions involving the error function. But it is simpler to calculate them numerically.

Appendix D

REMARKS ON THE NUMERICAL PROCEDURE

In calculating the matrix elements $\langle \mathring{\psi}_{\nu_1}|V_{corr}|\mathring{\psi}_{\nu_2}\rangle$, the integration over the coordinate z is performed numerically with the Simpson method. For small values of the dimensionless variables ξ, η, ζ (see appendix B), the wave functions $\varphi(z)$ are obtained from rapidly converging series expansion. For large values of $|\xi|$ or $|\zeta|$, asymptotic expansions are used (HMF 19.8.1). In the remaining range of ξ (and ζ), the wave functions $\varphi(z)$ are obtained by an extrapolation procedure starting from the asymptotic solutions and using the differential equation in the form of a difference equation.

The time needed for calculating a given number of matrix elements in our basis $\mathring{\psi}_\nu$ is larger than if we calculated them in the basis of eigenfunctions of a deformed harmonic oscillator. The reason is that all the eigenfunctions of the deformed harmonic oscillator can be generated from the lowest eigenfunctions by the use of recursion relations. In our case, this procedure is possible only for the ρ- and ϕ-dependent part of the basis functions $\mathring{\psi}_\nu$.

On the other hand, as already mentioned, the advantage of using the basis of eigenstates of H_0 [eq. (7)] is that these basis functions can describe arbitrarily large deformations up to the final separation of fragments, for instance also a strong constriction in the central part. If one wants to describe strongly constricted shapes in terms of eigenfunctions of a deformed harmonic oscillator, one has to include the more basis functions the more the potential shape deviates from a deformed oscillator.

For diagonalizing V_{corr} we use all states up to an energy $\approx \varepsilon_F + 30$ MeV ($\varepsilon_F =$

Fermi energy). This number of states is fairly constant for all nuclear shapes which can be assumed within our model. Since the largest part of the computer time is used for the diagonalization of the single-particle Hamiltonian, this advantage of the method appears to be important. We think that the functions $\overset{\circ}{\psi}_\nu$ which were explicitly given in appendix B, could provide a useful system of basis functions for obtaining the eigenfunctions of a strongly constricted Saxon-Woods potential and for carrying out Hartree-Fock calculations for strongly deformed nuclei.

References

1) N. Bohr and J. A. Wheeler, Phys. Rev. **56** (1939) 426
2) S. Frankel and N. Metropolis, Phys. Rev. **72** (1947) 914
3) S. Cohen and W. Swiatecki, Ann of Phys. **19** (1962) 67; **22** (1963) 406
4) V. M. Strutinski, JETP (Sov. Phys.) **18** (1964) 1298;
   V. M. Strutinski and A. S. Tyapin, JETP (Sov. Phys.) **18** (1964) 644
5) H. v. Groote and E. Hilf, Nucl. Phys. **A129** (1969) 513
6) W. D. Myers and W. Swiatecki, UCRL–11980. May 1965; Nycl. Phys. **81** (1966) 1
7) V. M. Strutinski, Nucl. Phys. **A95** (1967) 420; Ark. Fys. **36** (1967) 629
8) P. A. Seeger and R. C. Perisho, Los Alamos Scientific Laboratory Report LA-3751 (1967)
9) V. M. Strutinski, Nucl. Phys. **A122** (1968) 1;
   M. Brack, J. Damgaard, H. C. Pauli, A. Stenholm-Jensen, V. M. Strutinski and C. Y. Wong, to be submitted to Rev. Mod. Phys.
10) S. G. Nilsson, J. R. Nix, A. Sobiczewski, Z. Szymanski, S. Wycech, C. Gustafson and P. Möller, Nucl. Phys. **A115** (1968) 545;
    S. G. Nilsson, C. F. Tsang, A. Sobiczewski, Z. Szymanski, S. Wycech, C. Gustafson, I. L. Lamm, P. Möller and B. Nilsson, Nucl. Phys. **A131** (1969) 1
11) H. J. Krappe and U. Wille, Physics and chemistry of fission (Symposium, Vienna, 1969) SM-122/96
12) J. R. Nix, private communication
13) M. Demeur and G. Reidemeister, Ann. de Phys. **1** (1966) 181
14) P. Holzer, U. Mosel and W. Greiner, Nucl. Phys. **A138** (1969) 241;
    D. Scharnweber, U. Mosel and W. Greiner, Phys. Rev. Lett. **24** (1970) 601
15) C. Y. Wong, Phys. Lett. **30B** (1969) 61
16) J. R. Nix, Further studies in the liquid drop theory of nuclear fission, UCRL-17958, July 1968; Nucl. Phys. **A130** (1969) 241
17) S. T. Belyaev, Mat. Fys. Medd. Dan. Vid. Selsk. **31**, no. 11 (1959)
18) F. Dickmann and K. Dietrich, Nucl. Phys. **A129** (1969) 241
19) S. G. Nilsson, Mat. Fys. Medd. Dan. Vid. Selsk. **29**, no. 16 (1955)
20) J. N. P. Lawrence, Phys. Rev. **139** (1965) B1227; Los Alamos Scientific Laboratory Report. LA-3774 (1967) unpublished
21) Handbook of mathematical functions (referred to as "HMF") ed. M. Abramowitz and I. A. Stegun (Dover Public., New York, 1965)
22) L. Pauling and E. B. Wilson, Introduction to quantum mechanics (McGraw-Hill, New York, 1935)
23) W. H. Shaffer, Rev. Mod. Phys. **16** (1944) 245
24) A. Messiah, Quantum mechanics (North-Holland, Amsterdam, 1961) chap. XII